Light Metals 2014
Edited by: John Grandfield
TMS (The Minerals, Metals & Materials Society), 2014

EFFECT OF CURRENT DENSITY AND PHOSPHORUS SPECIES ON CURRENT EFFICIENCY IN ALUMINUM ELECTROLYSIS AT HIGH CURRENT DENSITIES

Rauan Meirbekova[12], Jomar Thonstad[2], Geir Martin Haarberg[2], Gudrun Saevarsdottir[1]
[1]Reykjavik University, School of Science and Engineering, Menntavegi 1, 101, Reykjavik (Iceland)

[2]Department of Materials Science and Engineering, NTNU, Sem Sælands vei 12, NO-7491, Trondheim (Norway)

Keywords: aluminum electrolysis, current efficiency, current density, phosphorus

Abstract

Effect of phosphorus on current efficiency for aluminum deposition was measured in a laboratory cell with current densities of 0.8 and 1.5 A/cm^2. Controlled amounts of $AlPO_4$ were added to the bath at the beginning of the experiment, and the effect on the current efficiency was studied at current densities of 0.8 A/cm^2 and 1.5 A/cm^2. Phosphorus levels were monitored through sampling the bath using High Resolution Inductively Coupled Plasma Mass Spectrometry at regular intervals during the whole electrolysis. The deleterious effect of phosphorus on the current efficiency was found to be pronounced at low concentrations up to 220 ppm. The current efficiency was found to increase with increasing cathodic current density and have a maximum current efficiency of 95.5% at 1.5 A/cm^2 for this particular cell design. A further increase of current density up to 2 A/cm^2 resulted in a decrease of current efficiency.

Introduction

A typical Hall-Heroult plant consists of many electrolytic cells connected in series carrying current of 150 – 400 kA DC. One of the main cost components in the operation of an aluminum smelter is electric power and the main parameter that signify operation quality in an aluminum smelter is current efficiency which is a measure of how efficiently electric current is used to produce aluminum in the cell [1].
The theoretical maximum is given by Faraday's laws and can be expressed with the following equation [2]:

$$P_{theoretical} = \frac{M}{zF} It \quad (1)$$

Where F= 96485 C mol^{-1} is Faraday's constant, *M* is the molar mass, z is the number of electrons involved in the electrode reaction, *I* is the current and *t* is the time. The current efficiency is the ratio between the actual mass of the metal produced and the mass theoretically derived from Faraday's law:

$$CE\% = \frac{P_{actual}}{P_{theoretical}} \quad (2)$$

The main mechanism for loss in current efficiency is the back reaction where metal dissolved in the bath reacts with CO_2 producing dissolved oxide and CO [3]. The back reaction where metallic aluminum dissolves in the electrolyte and is oxidized is written as:

$$2Al_{(diss)} + 3CO_{2(g)} = Al_2O_{3(diss)} + 3CO_{(g)} \quad (3)$$

Impurities in the electrolyte also represent a contribution to current efficiency loss. Phosphorus is a well-known example of how impurities can have a negative effect on current efficiency. The influence of phosphorus on current efficiency has been presented by a number of authors [4,5,6]. Current efficiency is reduced due to that phosphorus in the bath can undergo several cyclic redox reactions in the cathode and anode/CO_2 interfacial layers before leaving the cell. Sterten et al. [4] derived a new current efficiency model and concluded that the rate limiting steps for the loss in current efficiency were mass transport of multivalent impurity cations, in addition to the diffusion of dissolved sodium and monovalent aluminum ions through the boundary layer at the cathode [7].
In previously published works [8,9] the authors have presented the effect of additions of phosphorus as a function of current efficiency and effect of increasing current density on current efficiency. This is a third paper in a series concerning current efficiency. Previous results and the goal of this paper are briefly summarized below.
In previous work [8, 9] tests were done to study the deleterious effect of phosphorus on current efficiency. The works of Solli [5] and Thisted [6] done at 0.8 A/cm^2 were used as a reference, and new experiments were done at a higher current density of 1.5 A/cm^2. Other parameters were chosen to match Solli and Thisted. According to these results, phosphorus in the bath was found to decrease current efficiency also at high current density and gave a similar decrease of CE by 0.81% per 100 ppm of added phosphorus.
During the experiments, there was a concern about how well the phosphorous levels were controlled. Therefore, after termination of each experiment, the bath was removed from the crucible and analyzed for phosphorus using ICP (Inductive Coupled Plasma). The phosphorus concentration in the bath measured by ICP showed that the phosphorus level was lower than the target amount from initial additions. This was expected, because we observed that lots of phosphorus-containing powder was expelled by nitrogen gas coming out of the furnace. Control experiments where samples were regularly taken from the bath during electrolysis have later confirmed that the concentrations derived from solidified bath were not representative due to segregation under solidification, and it was concluded that depletion of phosphorous from the bath during the course of these experiments could be neglected.

Experimental Set-up

The experimental cell is located in a laboratory at NTNU/Sintef in Trondheim, Norway, and is similar to that of Solli [10]. The cell is

used to determine current efficiency for aluminum production during constant current electrolysis. Figure 1 is a schematic illustration of the cell. The advantage of this type of cell is that it provides a good convective pattern and maintains an almost flat cathode surface by using the graphite anode with holes drilled perpendicular to each other and a steel cathode which is wettable by liquid aluminum.

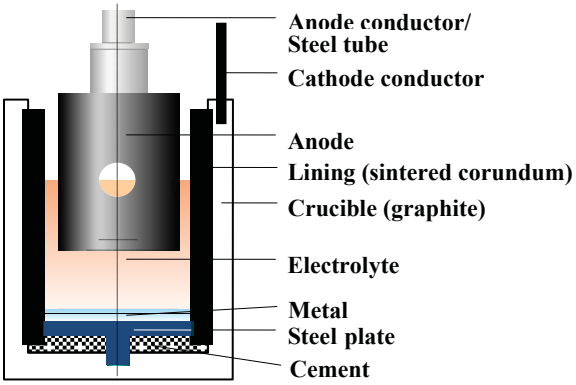

Figure 1. Schematic illustration of the laboratory cell.

First, a sintered alumina cylinder with diameter of 65 mm and length of 110 mm is placed inside a graphite crucible. The graphite crucible with a sintered alumina lining serves as the container for the molten electrolyte. Then, a steel pin 8 mm in diameter and 4 mm long is glued by carbon glue to the bottom of the crucible. This pin helps to provide electrical contact between the steel cathode and the graphite crucible. Afterwards, the bottom of the crucible is cemented with cast alumina cement (Termomax, Borgestad Fabrikker, containing 96 wt% of alumina 3 wt% CaO) and left to dry inside a 200 °C hot furnace for 2 days. Alumina powder is then poured on top of the dehydrated cement. These layers should prevent aluminum contact with graphite crucible, which can result in aluminum loss and aluminum carbide formation. Next, a steel plate with diameter of 60 mm and thickness of 5 mm is put on top of the alumina powder to act as a wettable material for the aluminum. At last, the prepared powder bath is poured on top of the steel plate. A bath is composed of AlF_3 (25,2 g), Na_3AlF_3 (319 g), CaF_2 (18,92 g), Al_2O_3 (15,13 g) corresponding to CR (molar ratio) of NaF/AlF_3 being 2.5, 4 wt% Al_2O_3 and 5 wt% CaF_2.

The cell is placed in a Pythagoras tube inside the furnace. Two ends of the tube are closed with copper plates, which are greased and sealed with rubber rings to ensure a gas tight furnace. The stainless steel tube is connected to the graphite anode with diameter of 52 mm and length of 70 mm and placed above the cell. The design of the anode fitted with vertical holes and horizontal channels is to facilitate convection in the cell. The bottom of the anode has 10° inclination up towards the center hole which will make gas bubbles move in the direction to the center hole.

Nitrogen gas is flushed with a flow rate of 0.2-0.3 dm^3/min through the furnace to prevent air burn of the cell. The system is water cooled where water is provided through tubes connected to the top and bottom of the furnace.

The thermocouple (Pt/Pt10Rh) is placed inside a slot of the crucible for the entire time of electrolysis and temperature readings are recorded. The temperature difference between the inside and outside of the bath is recorded in the first experiment and the temperature is regulated accordingly. Moreover, voltage and current readings are also monitored and recorded. The current is supplied by a DC power supply. The cathodic current density is calculated by the total current divided by the cross-sectional area of the sintered alumina lining using the inner radius. The cross sectional area of sintered alumina is equal to 33.17 cm^2. The furnace is connected to the electrical heater and the temperature is regulated by this heater. When the furnace has reached a temperature of 980°C, the anode is immersed in the bath until electrical contact is achieved. The immersion of the anode is repeated several times, and the contact points are marked on the steel tube. When the actual contact position is established, the anode tube is lowered an additional 2 cm from the contact position. Alumina additions are made manually every 15 min through a central steel tube penetrating the anode, and sampling of the bath was carried at constant intervals for each experiment.

The duration of each experiment is aimed at producing the same amount of aluminum, so at high current densities, and corresponding high total cell current, the duration would be shorter than at low current densities. The length of the experiment therefore ranges from 2-4 hours. After termination of the electrolysis, everything is switched off and left to cool down. Then the crucible is broken and aluminum is cleaned mechanically and left in an aqueous solution of $AlCl_3 \cdot 6H_2O$ at 25°C for 30 minutes. Current efficiency is calculated by weighing the amount of deposited aluminum and comparing it to the theoretical amount calculated from Faraday's law. Estimated loss because of handling the metal is assumed to be 0.9%.

Results and Discussion

Effect of Current Density

Experiments were carried out with Na_3AlF_6-Al_2O_3 (sat) with excess AlF_3 corresponding to CR (molar ratio of NaF/AlF_3) being 2.5 and 5 wt% CaF_2 at 980 °C.

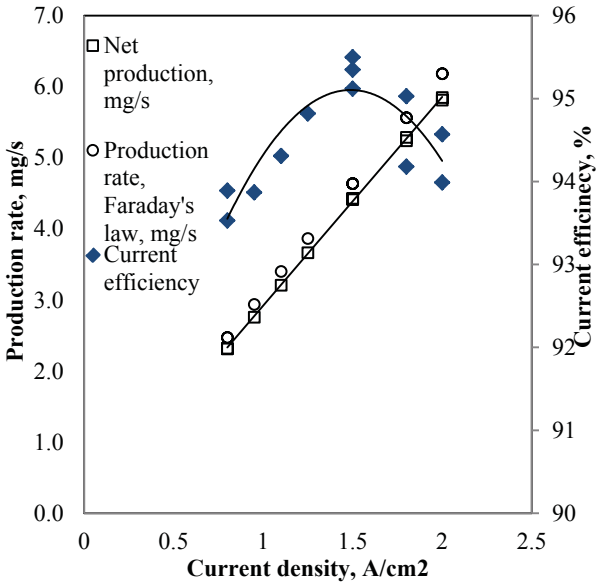

Figure 2. Illustration of the initial rate of formation of aluminum according to Faraday's law, the net rate of formation taking into account the current efficiency versus current density.

Figure 2 shows increased current efficiency with increasing current density up to 1.5 A/cm^2. A further increase in current

density is followed by a decrease of current efficiency even though the net rate of production still keeps increasing.

This behavior could be explained by two competing effects: the increased total current due to higher current density will increase metal production, while the rate of the back reaction is controlled by mass transfer and should remain similar unless other conditions are changed. This is counteracted by the fact that increased current density leads to increased stirring due to fluid dynamic effects and enhanced bubble formation. Increased flow rate leads to a thinner boundary layer which gives faster mass transfer and an increased rate of reoxidation of metal. The concentration overvoltage is dependent on the cell design and on the convection pattern in the cell and thus could be reduced substantially by the stirring of the melt [1]. Polyakov et al. [11] pointed out that interfacial stirring between metal and the electrolyte has significant effect on the current efficiency in aluminum electrolysis. Increased gas evolution at high current densities contributes in the same direction.

It should be noted that the noise from bubbling was more pronounced at cathodic densities ranging from 1.8-2 A/cm^2 which indicated presence of larger gas bubbles. Haupin and McGrew [12] observed that the gas bubble size was enlarged by increasing current density. Similar behavior is observed in Figure 2, where the data obtained by Solli [5] are plotted. However, the inclination of the curve starts after 1.1A/cm^2

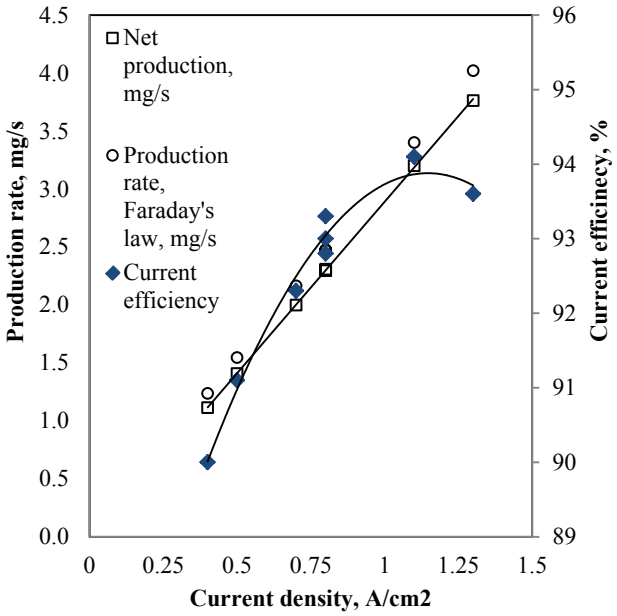

Figure 3. Illustration of the initial rate of formation of aluminum according to Faraday's law, the net rate of formation taking into account the current efficiency (CE) found for the current efficiency values for Solli‘s results [5].

The data presented in Figure 2 is listed in Table I. It is apparent that the rate of reoxidation increases with increasing current density. The same trend is seen in Table II, which lists data from Solli´s study shown in Figure 3. Rolseth and Thonstad have found that the rate of CO formation increases with increased stirring rate [13].

Table I. Rates of both metal production and reoxidation increase as a function of current density. The data is calculated by using the present study current efficiency values.

Data is calculated from present study				
CD	Theory	Net production	Rate of reox.	CE
A/cm2	mg/s	mg/s	mg/s	%
0.8	2.474	2.323	0.151	93.89
0.8	2.474	2.314	0.160	93.53
0.95	2.938	2.758	0.180	93.87
1.1	3.401	3.208	0.194	94.31
1.25	3.865	3.665	0.200	94.82
1.5	4.639	4.413	0.226	95.12
1.5	4.639	4.430	0.209	95.5
1.5	4.639	4.423	0.216	95.35
1.8	5.566	5.242	0.324	94.18
1.8	5.566	5.290	0.277	95.03
2	6.185	5.850	0.336	94.57
2	6.185	5.814	0.372	93.99

* CD-current density, Theory-theoretical production rate of aluminum according to Faraday‘s law, Net production- net rate of production taking into account the current efficiency, Rate of reox.- the rate of reoxidation, assuming that the rate of formation is 100% effective, CE-current efficiency.

Table II The rate of reoxidation increases as a function of current density. The data is calculated by using Solli´s current efficiency values [5].

Data is calculated from Solli's CE points				
CD	Theory	Net production	Rate of reox.	CE
A/cm2	mg/s	mg/s	mg/s	%
0.4	1.237	1.113	0.124	90
0.5	1.546	1.409	0.138	91.1
0.7	2.165	1.998	0.167	92.3
0.8	2.474	2.308	0.166	93.3
0.8	2.474	2.301	0.173	93
0.8	2.474	2.296	0.178	92.8
1.1	3.401	3.201	0.201	94.1
1.3	4.020	3.763	0.257	93.6

* CD-current density, Theory-theoretical production rate of aluminum according to Faraday‘s law, Net production- net rate of production taking into account the current efficiency, Rate of reox.- the rate of reoxidation, assuming that the rate of formation is 100% effective, CE-current efficiency.

The effect of Phosphorus

The predetermined amount of phosphorus was mixed with the bath contents before the start of the experiment. Samples for ICP analyses were taken at constant intervals during the experiment. Figures 4 and 5 illustrate how phosphorus concentration changes with time for different input contents. It was found that extra additions of phosphorus were not required. The amount of phosphorus added initially into the bath dropped to some extent in the beginning, but afterwards it remained stable for the whole period. Later, only first and last samples were analyzed by ICP

and if there was necessity other samples taken between were analyzed to find right concentration in the bath.

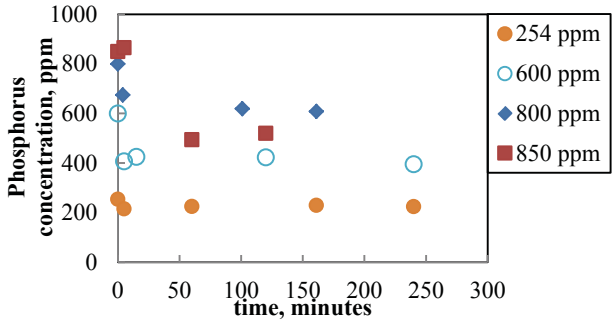

Figure 4. Phosphorus concentration change with time for different concentrations added in the beginning of the experiment.

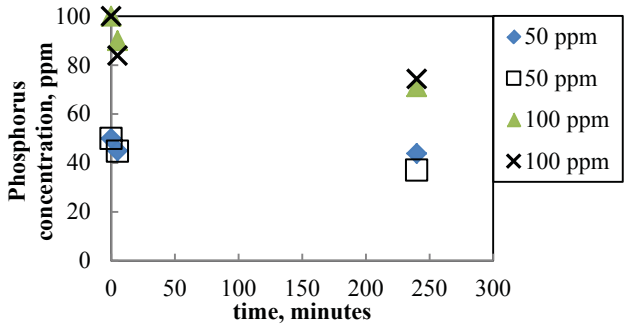

Figure 5. Phosphorus concentration change with time for different concentrations added in the beginning of the experiment.

The results given in Table III show the average concentrations in the bath measured by ICP as well as the initial amount of phosphorus in the mix.

Table III. The average concentrations in the bath measured by ICP at the different inputs of phosphorus.

Input	Average concentration in bath
ppm	ppm
50	41
50	39
100	80.6
100	79.1
254	223
254	230
600	412
800	634
800	626

As was mentioned in the introduction, the concentrations analyzed from bath samples taken after solidification were not representative due to segregation during solidification (Please compare Table III to Table IV)

Table IV. The concentrations in the bath measured by ICP at the end of the experiment from solidified bath.

Input	Concentration in solidified bath
600	96.3
800	244

By plotting the data presented in table III, a plot of average concentration in the bath as a function of the initially added amount can be constructed, which could be used to predict the expected concentration of phosphorus for a given amount added (Figure 6).

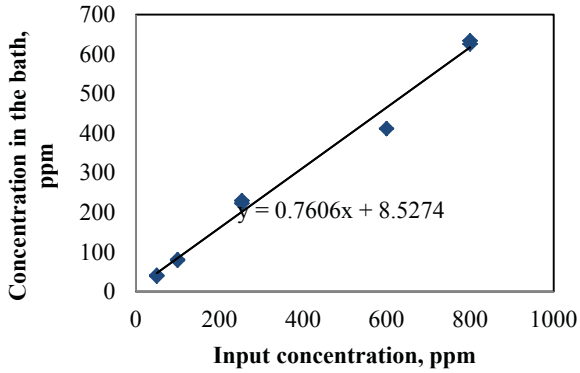

Figure 6. Average concentration of phosphorus in the bath analyzed by ICP at each input concentration.

The current efficiency as a function of the average phosphorus concentration is presented graphically in Figures 7 and 8. Tests with different concentration of phosphorus in the bath were run both at 0.8 A/cm^2 and 1.5 A/cm^2.

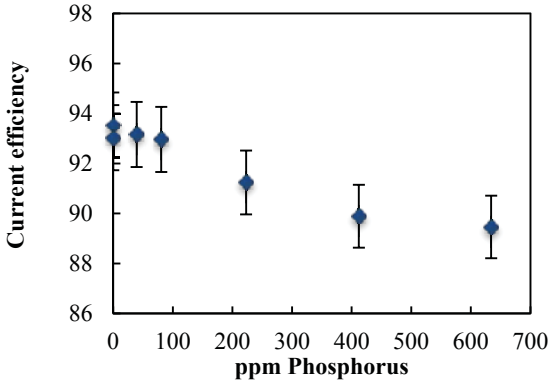

Figure 7. Current efficiency for aluminum deposition as a function of phosphorus at 0.8 A/cm^2. The error bars were constructed using the percentage of error in experiments to be 1.4% as used by Solli [5].

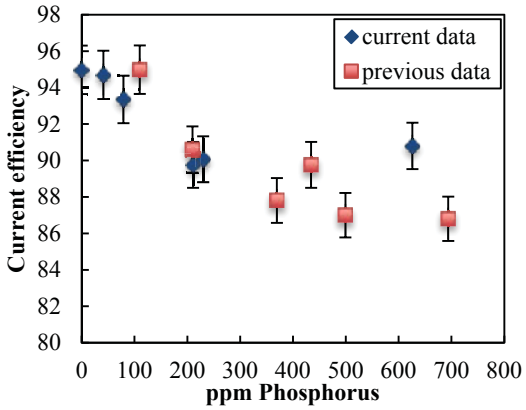

Figure 8. Current efficiency versus phosphorus concentration in the bath for the current study and the previous study with corrected values using Figure 6 at 1.5 A /cm^2. The error bars constructed using percentage of error in experiments to be 1.4% as used by Solli [5].

The slope of current efficiency as a function of phosphorus concentration up to 630 ppm was calculated by least square fit and corresponds to 0.67% ±0.07 per 100 ppm of phosphorus at 0.8 A/cm^2. (P-value corresponds to 0.0003).

By using Figure 4 we can correct results obtained from earlier experiments for the current density of 1.5 A/cm^2 [8] and combine them with new results from current study as shown in Figure 8. Figure 8 shows that the effect of phosphorus is gradual and seems to level off eventually at higher concentrations. Current efficiency reduction for the range of concentration up to 630 ppm is found to be 1.06% ±0.31 per 100 ppm phosphorus. (P-value is equal to 0.007).

Other authors [6,13] have reported that the effect of phosphorus on current efficiency at higher concentrations becomes constant. Keppert [14] commented on Solli´s work that this phenomenon was observed at above 330 ppm whereas Thisted [6] reported it after 500 ppm. Both of them anticipated that this could be due to higher evaporation of phosphorus species at higher levels. In Table III, it is clear that at higher concentrations there is higher drop in concentration of phosphorus. Although the statistical error does not allow us to state with confidence that the effect of phosphorous on current efficiency is nonlinear, the tendency is there, which supports previous findings.

Regression analysis of current efficiency as a function of phosphorous content at levels up to 220 ppm gives a reduction of 2.41% ±0.45 per 100ppm of phosphorus at 1.5 A/cm^2. Doing the same for a lower current density (0.8 A/cm^2) the slope of 0.92% ±0.16 per 100 ppm of phosphorus was obtained. The slopes were calculated by least square fit method, and the P-values for the current density of 1.5 A/cm^2 and 0.8 A/cm^2 are 0.003 and 0.01 respectively.

The presumption that the effect of phosphorus might be less important at higher current densities was not confirmed for this cell, and the results indicate that on the contrary the effect of phosphorus is more pronounced at higher current density. This can possibly be attributed to increased stirring due to bubble formation and fluid dynamic effects, which lead to thinner diffusion layers and therefore more efficient mass transfer to the reaction planes. Thus, cyclic redox reactions are enhanced at higher current densities.

Alternatively the larger effect of phosphorus at high current densities may be explained in terms of changing the cathode potential. A higher current density leads to a higher cathodic overvoltage, which means that the potential for formation of P(3-) species can be reached. The possible formation of P(3-) will cause a more significant loss in the current efficiency due to cyclic reduction of P(5+) and oxidation of P(3-).

Conclusion

Measurements of current efficiency as a function of cathodic current density showed that for this particular laboratory cell, increasing cathodic current density above 1.5 A/cm^2 lowers the current efficiency. This slight decrease is most likely caused by increase in gas evolution and fluid dynamic stirring, which affects the diffusion boundary layer and enhances mass transfer. However, one should note that the shape of the curve produced in this paper is dependent on the apparatus used and the reduction of current efficiency above 1.5A/cm^2 might not be the case for other cell designs with different flow patterns. The basic principles should however be the same, thus at a certain point the reduction of current efficiency is expected caused by faster fluid flow and more efficient mass transfer, speeding up the back reaction.

Analyses of bath samples taken at constant intervals during the whole electrolysis period revealed that phosphorus stays more or less constant in the bath through the duration of the experiment, and regular additions are not necessary. Based on this analysis a plot was made which can be used to determine the average phosphorus concentration in the bath depending on the input amount.

It was found that the effect of phosphorus on the current efficiency is much more pronounced at higher current density and at relatively low phosphorus contents up to 220 ppm, giving a reduction of 2.41% ±0.45 per 100ppm of phosphorus at 1.5 A/cm^2 compared to 0.8 A/cm^2 which gave 0.92% ±0.16 per 100 ppm of phosphorus for the same range of the concentration**.**

Error Bars in Determined CE

The percentage of error was set at 1.4% for the error bars. This number is the sum of most important sources of error estimated by Solli [5]. He wrote that 1.4% should give worst case scenario for experimentally determined current efficiency. Table V shows only values for the source of errors, and the details of each of them are described in Solli´s thesis [5].

Table V. Sources of error

Source of error	Error	Error in CE
Temperature	±4 K	±0.4
Cleaning, weighing metal	±0.1 g	±0.3
Current	±0.02 A	±0.1
Metal Surface Area/current density	±2 cm^2 ±0.05 Acm^2	±0.3
bath ratio		-0.1-0.3

Acknowledgements

Assistance from Petre Manolescu and Joseph Prince Armoo is gratefully acknowledged.

References

1. J. Thonstad, P. Fellner, G.M. Haarberg, J. Híveš, H. Kvande, and Å. Sterten *Aluminum electrolysis – Fundamentals of the Hall-Héroult process*, 3rd edition (Aluminum-Verlag GmbH, Düsseldorf, Germany, 2001), 227
2. K. Grjotheim and H.Kvande, Introduction to Aluminum Electrolysis, (Aluminum-Verlag GmbH, Düsseldorf, Germany, 1993), 147
3. K. Grjotheim , C. Krohn, M. Malinovsky, K. Matiasovsky, and J. Thonstad, *Aluminum electrolysis – Fundamentals of the Hall-Héroult process*, 3rd edition (Aluminum-Verlag GmbH, Düsseldorf, Germany, 1992)
4. Å.Sterten, P.A. Solli, and E. Skybakmoen, Influence of electrolyte impurities on current efficiency in Aluminum electrolysis cells, J. Appl. Electrochem., 28, 781 (1998)
5. P.A. Solli, *Current efficiency in Aluminum electrolysis cells*, (Ph.D. thesis, Norwegian University of Science and Technology, 1993), 116-128.
6. E.W. Thisted, Electrochemical properties of Phosphorus Compounds in Fluoride Melts cells, (Ph.D. thesis, Norwegian University of Science and Technology, 2003), 200-202
7. P.A. Solli, E. Skybakmoen, and Å.Sterten, Current Efficiency in the Hall-Héroult process for Aluminum electrolysis: experimental and modeling studies, J. Appl. Electrochem., 27, 939-946 (1997)
8. R. Meirbekova, G. Saevarsdottir, J.P. Armoo and G.M. Haarberg, Effects of current density and phosphorus impurities on the current efficiency for Aluminum deposition in cryolite-alumina melts in a laboratory cell, In proceedings, Molten Salts 9, Trondheim June 2011.
9. R. Meirbekova, G. Saevarsdottir, J.P. Armoo and G.M. Haarberg, Effects of current density and phosphorus impurities on the current efficiency for Aluminum deposition in cryolite-alumina melts in a laboratory cell, Light Metals 2013,The Metals Materials and Mineral Society
10. P.A. Solli, E. Skybakmoen, and Å.Sterten, Design and performance of a laboratory cell for determination of current efficiency in the electrowinning of Aluminum, J. Appl. Electrochem., 26, 1019-1025 (1996)
11. P.V.Polyakov, V.Y. Buzunov, Y.G. Mikhaev and V.G.Printsev, Movement of Metal-Electrolyte Interface in Aluminum Reduction cells by Marangani Effect, Tsvetnye Metally, Vol.34, No 3, 29-31, 1993.
12. W.Haupin and W. McGreew, Aluminium 51, 273, 1975
13. S. Rolseth. and J. Thonstad, On the mechanism of the Reoxidation Reaction in Aluminum Electrolysis, Light Metals 1981,The Metals Materials and Mineral Society, 289-301
14. M.Keppert, Electrochemical behaviour of the phosphorus species in fluoride melts, (Ph.D. thesis, Norwegian University of Science and Technology, 2006), 20